Joint Time-Frequency-Space Transmitter Analytics via Dictionary-Based Tensor Factorization

Blessing Okoro, Petko Bogdanov, Mariya Zheleva
Department of Computer Science, University at Albany, State University of New York, USA.
{aaokoro, pbogdanov, mzheleva}@albany.edu

***Abstract*—Traditional spectrum analytics focus either on transmitter time-frequency characterization or localization. Solving these tasks in isolation limits the methods' applicability to complex real-world scenarios where both time-frequency and spatial awareness are critical for sharing and enforcement. In addition, the potential accuracy gains from joint characterization and localization have not been explored. To address these gaps, we propose `MDL` (Multi-vantage Detection and Localization), a framework for joint transmitter characterization across time, frequency, and space using multi-vantage-point traces. We model multi-sensor spectrum measurements as a three-way tensor, where slices represent Power Spectral Density (PSD) data from individual sensors. We employ sparse dictionary-coding with appropriate analytical dictionaries for the temporal, spatial and frequency modes to decompose the input tensor and utilize the extracted factors for characterization and localization. Our method simultaneously estimates time-frequency occupancy patterns and a proxy Received Signal Strength (RSS) for multiple transmitters, enabling joint detection, separation and localization. In evaluation `MDL` achieves up to 25% accuracy improvement over baselines for time-frequency characterization and enables 2x to 12x reduction of the localization error when combined with state-of-the-art localization techniques. It also enables more accurate detection of the number of transmitters in a trace compared to alternatives.**

***Index Terms*—spectrum sensing, transmitter detection, characterization, localization, sparse dictionary coding.**

I. Introduction

Spectrum measurement and analytics are essential for emerging spectrum-sharing policy and technology. Analytics seek to answer a plethora of questions from a spectrum trace: (i) how many transmitters are present, (ii) what is their temporal/frequency behavior, (iii) where in space are they located, (iv) are they moving and (v) what modulation are they using. Each of these problems has been tackled independently, and in turn, requires a different measurement strategy to be solved. For example, transmitter counting and temporal/frequency characterization can be obtained using a wideband spectrum scan [1], [2], and are thus generally considered technology-agnostic. However, localization and modulation recognition tend to be technology-aware, and with a few exceptions [3] require exact knowledge of the target transmitter's properties (e.g. bandwidth and operational frequency) for data collection [4], [5], [6]. This makes it impossible to answer multiple questions from the above using a single measurement campaign.

Our work lays the foundation of *multi-objective analytics*, whereby a single wideband measurement campaign can be used to answer multiple questions about spectrum occupancy. In this work we focus on the following targets: (i) transmitter counting, (ii) per-transmitter time-frequency characterization and (iii) localization, which are achieved in a single-shot tensor factorization framework. Our method is designed for multi-vantage-point spectrum measurements, where a number of sensors are deployed throughout an area to concurrently observe spectrum activity (left pane of Fig. 1). Given this measurement infrastructure, our goal is to detect the number of active transmitters, their temporal and frequency behavior and their location, thus providing a holistic view of the space-time-frequency spectrum occupancy in a given area.

Related work can be grouped as follows: (i) time-frequency transmitter detection and characterization; (ii) single- and multi-transmitter localization, (iii) cooperative sensing and (vi) sparse dictionary coding. First and foremost, existing characterization and localization methods [7], [8], [9], [1], [2], [10] focus on their single respective task, whereas our work seeks to jointly characterize the time-frequency activity and localize all active transmitters. Prior *transmitter characterization* work estimates the number of observed transmitters in a wide-band trace and performs per-transmitter detection of time-frequency activity [1], [2], [10]. Methods in this category employ a single vantage point measurement, whereas `MDL` fuses data from multi-sensor traces to maximize characterization accuracy.

Prior *localization* methods tackle single- [5], [6], [11] and multi-transmitter [3], [12], [7], [13] scenarios. Some are supervised [7], [13], while the majority are unsupervised [3], [12], [7]. All of these works are technology-aware, i.e., they require the exact transmitter bandwidth to be known apriori and measured in full without extraneous noise or other transmitters. In contrast, our work supports transmitter-agnostic localization, whereby a target may be measured alongside noise and other transmitter activity. Furthermore, our work is orthogonal to all prior RSS based localization literature. We provide an efficient way to extract a proxy transmitter power measure from multi-vantage and technology-agnostic traces, which can then be used as an input to any pre-existing RSS based localization method, as demonstrated in our evaluation §III.

Cooperative sensing employs multiple senors that jointly measure the spectrum for occupancy analytics. Traditional approaches define the problem as a binary hypothesis testing where the objective is to determine if a primary user is present or not [14]. This problem has more recently been revisited in the context of deep cooperative sensing [15] and federated

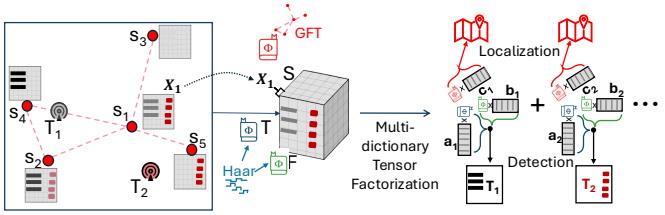

Figure 1: Overview of MDL for multi-vantage spectrum analytics. *Left panel:* a sensor network of 5 sensors s_1 to s_5 observing transmitters T_1 and T_2 across a spatial area where each sensor collects time-frequency traces. *Middle panel:* Data from all sensors modeled as a 3-way time-frequency-space tensor formed from the individual sensor measurements, and modality-specific dictionaries for each tensor mode. *Right panel:* joint characterization using dictionary-based decomposition where each component corresponds to a transmitter. Time/frequency characterization is obtained from the time $\mathbf{\Phi}_1\mathbf{a}_i$ and frequency $\mathbf{\Phi}_2\mathbf{b}_i$ mode vectors, while the spatial mode vector $\mathbf{\Phi}_3\mathbf{c}_i$ is utilized for localization.

cooperative sensing [16], where the objective remains the same, and the effort is on improving accuracy while reducing the computational cost and preserving privacy. Beyond simply testing if a primary user transmits, we seek a more granular characterization of the spectrum activity, including the number of active transmitters and their time-frequency-space characteristics. This tasks has not been tackled in prior cooperative sensing literature. Finally, our methodology is rooted in *sparse dictionary coding* [17] which is central to signal processing, machine learning and data analytics with applications in multiple fields. Spectrum scans, albeit noisy, allow for inherently sparse representation via an appropriate dictionary basis. So far [2] has employed a sparse dictionary framework for single-vantage point transmitter characterization, but multi-vantage-point analytics that tackle joint characterization and localization have not been explored. Note that related work also exists on supervised classification of transmitter technology [18]. Our work is orthogonal, as it seeks to discern transmitter activity with high granularity and sensitivity, but does not target technology classification.

We propose MDL (Multi-vantage Detection and Localization), which takes PSD measurements over time $\mathbf{X} \in \mathbb{R}^{T\times F}$ from multiple sensors $s \in S$ in the form of a 3-way tensor $\mathcal{X} \in \mathbb{R}^{T\times F\times S}$ (Fig. 1 middle). MDL employs a dictionary-based tensor decomposition to isolate transmitters into separate components. Unlike classical canonical polyadic decomposition (CPD) [19], each component vector is represented as a sparse combination of mode-appropriate analytical dictionary atoms: Haar wavelets are used for the time and frequency modes, and the Graph Fourier Transform for the spatial mode. The resulting component vectors are employed to detect individual transmitters across time, frequency, and space (Fig. 1 right panel).

Our paper makes the following contributions:

- **Novelty:** We design MDL, the first framework for joint transmitter detection, characterization and localization from wide-band technology-agnostic traces, which employs efficient sparse multi-dictionary coding.
- **Accuracy:** Compared to baselines, MDL achieves up to 25% accuracy improvement in time-frequency characterization, 2x to 12x reduction of localization error, and enables more accurate detection of the number of active transmitters.
- **Applicability:** MDL is unsupervised and computationally lightweight and is, thus, applicable across various practical scenarios and with arbitrary coexisting technologies.

II. Methodology

A. System model and Preliminaries

We consider a spectrum monitoring scenario where S sensors are spatially distributed across a two-dimensional area to perform coordinated spectrum sensing. Each sensor has a wideband sensing capability to collect spectrum traces across a designated frequency range. We assume that all sensors perform spectrum scans simultaneously across the same frequency band, ensuring spatial and temporal alignment of the collected data from the sensor network.

The input to our framework is a 3-way tensor of PSD $\mathcal{X} \in \mathbb{R}^{T\times F\times S}$ data, representing spectrum measurements at S sensors over T time steps and F frequency bins. A frontal slice $\mathbf{X}_s \in \mathbb{R}^{T\times F}$ corresponds to the PSD measurement at sensor s. We model $\mathbf{X}_s$ as a mixture of the power footprint of b_s transmitters $\mathbf{T}_i$ that are observable from sensor s and independently and identically distributed (i.i.d.) Gaussian noise ϵ:

$$\mathbf{X}_s = \sum_{i=1}^{b_s} \mathbf{T}_i + \epsilon. \tag{1}$$

Note that the same transmitter $\mathbf{T}_i$ may be observable from multiple sensors, with varying signal to noise ratio (SNR). For example, in Fig. 1 T_1 has the highest SNR at s_4, lower SNR at s_2 and s_1 and not observable at s_3 and s_5. This multi-vantage observation of the same transmitter presents an opportunity to improve its detection in noisy regimes over observing from a single sensor. To achieve this, the characterization has to be done simultaneously from all slices. This intuitive goal aligns with tensor decomposition, where factors in widely adopted models like canonical polyadic decomposition (CPD) [20] capture regularities across modes in individual components. Intuitively our goal (through the lense of tensor decomposition) is to extract each transmitter as a rank-1 component of a tensor factorization model (Right pane of Fig. 1). CPD expresses $\mathcal{X}$ as a sum of R rank-one tensors:

$$\mathcal{X} = \sum_{r=1}^{R} \mathcal{X}_r = \sum_{r=1}^{R} \mathbf{a}_r \circ \mathbf{b}_r \circ \mathbf{c}_r \tag{2}$$

where $\circ$ denotes the tensor outer product, $\mathcal{X}_r$ are rank one tensors obtained from outer tensor product of the r-th component $\mathbf{a}_r \in \mathbb{R}^T$, $\mathbf{b}_r \in \mathbb{R}^F$, and $\mathbf{c}_r \in \mathbb{R}^S$. A shorthand notation for this decomposition $\mathcal{X} = [[\mathbf{A}, \mathbf{B}, \mathbf{C}]]$ can be obtained by stacking R component vectors $\mathbf{a}_r$, $\mathbf{b}_r$ and $\mathbf{c}_r$ into corresponding factor matrices. While CPD captures low-rank structure, it does not leverage prior knowledge about the underlying signal characteristics. For example, we know that transmitters occupy contiguous frequency bands, their on/off activity in time spans contiguous time steps and their

perceived power at individual sensors varies smoothly as a signal over a distance-weighted graph representing the sensor network spatially. To incorporate this prior knowledge from the domain we adopt a dictionary-based decomposition [21] in which components in every mode are represented as sparse encoding through appropriately defined dictionaries $\mathbf{\Phi}$. The dictionary-based decomposition is defined similar to CPD:

$$\mathcal{X} = \sum_{r=1}^{R} \mathbf{\Phi}_1 \mathbf{a}_r \circ \mathbf{\Phi}_2 \mathbf{b}_r \circ \mathbf{\Phi}_3 \mathbf{c}_r = [[\mathbf{\Phi}_1 \mathbf{A},\ \mathbf{\Phi}_2 \mathbf{B},\ \mathbf{\Phi}_3 \mathbf{C}]], \quad (3)$$

where $\mathbf{\Phi}_i$ are the dictionaries for the time, frequency and space modes and the factors $\mathbf{A}, \mathbf{B}$ and $\mathbf{C}$ are sparse, i.e. only a few elements of vectors $\mathbf{a_r}, \mathbf{b_r}, \mathbf{c_r}$ are non-zero. This formulation offers several advantages: (1) incorporation of domain priors through a careful design of the dictionaries $\mathbf{\Phi}_i$; (2) improved robustness in low-SNR regimes due to the structured and sparse representation; and (3) improved interpretability and clear separation of transmitters' time-frequency activities and spatial signatures. We next describe the overall `MDL` procedure and the dictionaries we adopt for our task.

Algorithm 1 `MDL` Algorithm

Require: Measurements $\mathcal{X} \in \mathbb{R}^{T \times F \times S}$, mode-specific dictionaries $\mathbf{\Phi}_1$, $\mathbf{\Phi}_2$, and $\mathbf{\Phi}_3$, max rank r_m, threshold β

Ensure: Transmitter activities $\mathbf{\Omega}_i$ and locations $(\mathbf{x}_i, \mathbf{y}_i)$.

1: *// 1: Dictionary-based factorization*
2: $\mathbf{\Phi}_1\mathbf{A}, \mathbf{\Phi}_2\mathbf{B}, \mathbf{\Phi}_3\mathbf{C} \leftarrow \text{MDTD}(\mathcal{X}, \mathbf{\Phi}_1, \mathbf{\Phi}_2, \mathbf{\Phi}_3, r_m)$ Eq. (3)
3: *// 2: Component selection*
4: **for** $r = 1$ to r_m **do**
5: $\quad \mathcal{X}_r \leftarrow \Phi_1 \mathbf{a}_r \circ \Phi_2 \mathbf{b}_r \circ \Phi_3 \mathbf{c}_r$
6: $\quad \mathbf{f}_r \in \mathbb{R}^F \leftarrow sum_{T,S}(\mathcal{X}_r)$ ▷ sum along T and S
7: $\quad \text{score}_r = count(\mathbf{f}_r^i \geq \beta \times \max(\mathbf{f}_r))$
8: **end for**
9: Retain $(\mathbf{a}_i, \mathbf{b}_i, \mathbf{c}_i)$ in higher $GMM(score, 2)$ component
10: *// 3: Detection and localization from retained components*
11: **for** $(\mathbf{a}_i, \mathbf{b}_i, \mathbf{c}_i)$ in retained components **do**
12: $\quad \mathbf{T}_i = (\mathbf{\Phi}_1\mathbf{a}_i)(\mathbf{\Phi}_2\mathbf{b}_i)^\top \in \mathbb{R}^{T \times F}$
13: $\quad \mathbf{\Omega}_i(l, m) = 1$ iff $\mathbf{T}_i(l, m)$ in higher component of $GMM(\mathbf{T}_i, 2)$ and 0 otherwise.
14: $\quad$ Location $(x_i, y_i) \leftarrow$ Localization$(\mathbf{\Phi}_3\mathbf{c}_i)$
15: $\quad$ Add $\mathbf{\Omega}_i$ and (x_i, y_i) to detected transmitters
16: **end for**

B. `MDL`: Multi-vantage detection and localization

Next we present the overall procedure of our framework `MDL` listed in Alg. 1. The input to our method is the measurement tensor $\mathcal{X}$ and dictionary matrices $\mathbf{\Phi}_i$ for the temporal, frequency and spatial mode which we define in the following section. Additionally, the method is parametrized by the maximum number of tensor factors to consider r_m which correspond to the maximum possible transmitter detected and a power threshold β used for component selection and discuss below. `MDL` performs joint time-frequency-space transmitter characterization and localization in three main steps: (1) Factorization (Steps 1-2), (2) Component selection (Steps 3-9) and (3) Detection and localization from selected components (Steps 10-16).

Factorization. The goal in the factorization step is to obtain sparse coded factors $\mathbf{A}, \mathbf{B}, \mathbf{C}$ for the input tensor given predefined dictionaries $\mathbf{\Phi}_i$. Formally, this step seeks to solve the following optimization problem:

$$\min_{\mathbf{A},\mathbf{B},\mathbf{C}} ||\mathcal{X} - [[\mathbf{\Phi}_1\mathbf{A}, \mathbf{\Phi}_2\mathbf{B}, \mathbf{\Phi}_3\mathbf{C}]]||_F^2 + \lambda_1 \|\mathbf{A}\|_1 + \lambda_2 \|\mathbf{B}\|_1 + \lambda_3 \|\mathbf{C}\|_1,$$

where the first term measures the fit between the factorization model to the input data using a tensor Frobenius norm and the following terms encourage sparsity in fitted factors via L_1 loss and parametrized by mode-specific sparsity parameters λ_i. A solution based on the alternating direction method of multipliers (ADMM) for this problem was recently proposed in the MDTD method [21]. We employ the solver and set $\lambda_i = 10^{-8}$ for all factors. This level of sparsity enables a good performance for `MDL` across transmitter SNR levels, however, we expect that higher sparsity parameters would benefit more noisy settings. We set the rank of the decomposition (number or columns in the factors $\mathbf{A}, \mathbf{B}, \mathbf{C}$) to r_m which is the maximum number of transmitters that can be detected in our data. We set this value sufficiently large in experiments (larger than the actual number of transmitters) and propose a way to select factors (components) which contain transmitters described next.

Component selection. `MDL` separates individual transmitters into distinct rank-1 components. Ideally, the decomposition rank r_m would be set to $b + 1$, where b is the number of transmitters and the additional component captures background noise. However, since the true number of transmitters is unknown *apriori*, we overestimate the rank by setting r_m to a large value and then apply the factor selection steps (Steps 3 to 9) to retain only a subset of factors that are likely to contain transmitters for downstream analysis.

To identify components containing a transmitter, we leverage the structural assumption that the encoded transmitter activity is consistent in the frequency bins of the transmitter across vantage points and time steps. As a result, if we aggregate the power observed in frequency bins over time and vantage points, it will have a significant number of high values (transmitter) compared to a factor that fits only noise and no transmitter. Following this intuition, we compute the reconstructed rank-1 tensor corresponding to candidate factor r (Step 5) and then aggregate the tensor along the time and spatial modes to obtain a *frequency profile* $\mathbf{f}_r \in \mathbb{R}^F$ (Step 6). Next, we compute a *frequency score* for the factor by counting the number of frequency bins $\mathbf{f}_r$ which exceed a high activity threshold $\beta = 0.85$ of the maximum f_r^i (Step 7).

Finally, we apply a two-component Gaussian Mixture Model (GMM) to cluster the frequency scores into transmitter (high value) and noise groups (step 9). This clustering is effective since transmitter-related components tend to have higher frequency scores due to their structured nature, while

noise components yield lower, less coherent scores. We retain components clustered as transmitters (high scores) and discard the rest.

Transmitter detection and localization in retained components. After selecting the relevant rank-1 tensor components, we proceed to characterize each transmitter's time and frequency activity, and then utilize the spatial mode factors for localization (steps 10 to 16). To compute the time frequency activity for each retained component i, we first compute the outer product of its time and frequency mode factors: $\mathbf{T}_i = (\mathbf{\Phi}_1\mathbf{a}_i)(\mathbf{\Phi}_2\mathbf{b}_i)^\top \in \mathbb{R}^{T\times F}$ step (step 12). The assumption is that the fitted component is denoised due to the dictionary priors and sparsity in the decomposition, so a simple clustering of the reconstructed values will highlight the time-frequency regions of transmission. Following this intuition, we create a binary mask $\mathbf{\Omega}_i$ using a two-component GMM of all reconstructed values to separate active transmission regions from inactive regions (Step 13). The binary mask indicates when and where the transmitter is active.

The third mode factor $\mathbf{\Phi}_3\mathbf{c}_i \in \mathbb{R}^S$ associated with each component serves as a proxy RSS vector. Namely, this vector captures the relative signal intensity observed across the sensor network nodes for the given transmitter component. Hence `MDL` produces spatial estimates for the perceived power at different sensors that can be directly fed into conventional power-based localization techniques (Step 14). Compared to traditional RSS measurements, which are collected from the receiver's perspective and depend on device-specific characteristics (e.g., gain, calibration, hardware variability), the proxy vector obtained through decomposition is entirely *device-agnostic* and obtained based on consensus among sensors about the time-frequency activity of the transmitter.

Also, most power-based localization methods are limited to localizing a single active transmitter at a time, as they operate on aggregated or ambiguous RSS measurements. In contrast, `MDL` separates overlapping transmissions into distinct components via tensor factorization. As a result, each transmitter is isolated into its own rank-1 factor, and the corresponding proxy vector $\mathbf{\Phi}_3\mathbf{c}_r$ can be used to localize that transmitter independently. As we demonstrate in experiments, this enables accurate *multi-transmitter localization* without requiring explicit knowledge of the number or identity of transmitters in advance.

C. Dictionary construction

Next we discuss the analytical dictionaries employed in `MDL`. To exploit structured priors in each tensor mode, we adopt fixed dictionaries that encode expected behavior in the temporal, spectral, and spatial domains. As shown in Fig. 1 wireless communication transmitters exhibits on/off switching behavior. The left panel of the figure shows transmitters T_1 and T_2 alternating between active and idle states across time, creating sharp transitions and piecewise-constant segments typical of communication systems. The same activity patterns are observed by all sensors at different SNRs. This bursty and localized nature of transmitter activity makes Haar wavelet dictionaries $\mathbf{\Phi}_1 \in \mathbb{R}^{T\times T}$ well suited for the temporal mode sparse coding, because they excel at representing localized, piecewise-constant signals and have been widely used in compressive signal representation [22], [23]. Likewise, T_1 and T_2 in Fig 1 exhibit contiguous spectral occupancy typical of communication systems, where each transmitter occupies a connected block of frequency bins rather than scattered spectral components. This sparse, contiguous frequency pattern also aligns well with Haar wavelet dictionaries $\mathbf{\Phi}_2 \in \mathbb{R}^{F\times F}$ which we also employ to succinctly represent sharp spectral boundaries and uniform power distribution within occupied bands.

In the multi-vantage-point deployment shown in Fig. 1's left panel sensors s_1 through s_5 are spatially distributed and observe transmitters from different locations with varying gains. Intuitively, the fitted spatial factors $\Phi_3\mathbf{c}_i$ corresponding to the transmitter should correspond to a smooth spatial signal over the sensor network. For the sensor mode, we construct a dictionary $\mathbf{\Phi}_3 \in \mathbb{R}^{S\times S}$ based on the Graph Fourier Transform (GFT) of the sensor network. We model the sensor network as an undirected weighted graph $\mathcal{G} = (V, E)$, where each node $v_i \in V$ represents a sensor, and edges $(v_i, v_j) \in E$ reflect proximity based on physical deployment. The edge weights w are defined using inverse distances: $w_{ij} = \frac{1}{p_{ij}}$ for $i \neq j$, where p_{ij} is the Euclidean distance between sensors i and j. We work with the top-k graph, i.e., we set all edges between nodes who are not among their top-k neighbors to 0. We use $k = 5$ for all experiments.

Let $\mathbf{A}$ be the weighted adjacency matrix of the top-k sensor graph and $\mathbf{D}$ the degree matrix (degree of a node is the sum of adjacent edge weights). The graph Laplacian is defined as: $\mathbf{L} = \mathbf{D} - \mathbf{A}$. The GFT basis $\mathbf{\Phi}_3$ is then obtained by computing the eigenvectors of $\mathbf{L}$: $\mathbf{L} = \mathbf{U}\mathbf{\Lambda}\mathbf{U}^\top$. Where $\mathbf{U}$ is a matrix of eigenvectors which forms the GFT basis $\mathbf{\Phi}_3$ and $\mathbf{\Lambda}$ is a diagonal matrix of eigenvalues. This basis captures smooth variations over the sensor graph, enabling us to represent transmitter power patterns that vary smoothly with respect to the spatial sensor layout.

III. Experimental evaluation

A. Experimental setup

Data. We evaluate `MDL` on a synthetically generated dataset designed to reflect realistic signal propagation and sensor behavior. The simulated sensor network is deployed over a $200\,\mathrm{m} \times 200\,\mathrm{m}$ area. Both sensor and transmitter coordinates are randomly sampled within this region, with the constraint that each deployment includes a mix of *active* sensors (those within sensing range of at least one transmitter) and *inactive* sensors (those outside the effective range of any transmitter). This setup mimics realistic heterogeneity in sensor coverage. We model the signal propagation using the *log-normal path loss* model: $P_r = P_t - 10\eta \log_{10} d + \gamma$ where P_r is the received power at a sensor, P_t is the transmitter power, d is the distance between the sensor and the transmitter, η is the path loss exponent, and γ captures shadowing effects. For our experiments we set $\eta = 3.5$ and $\gamma = 5$.

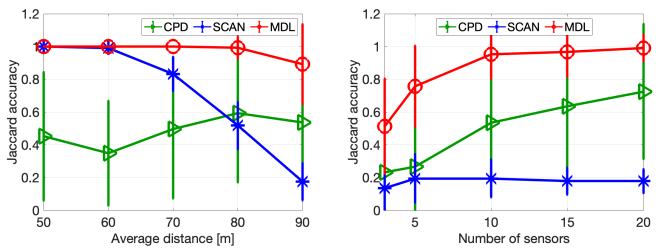

Figure 2: Characterization accuracy with increasing average distance between transmitters and sensors (left); and increasing sensor density (right).

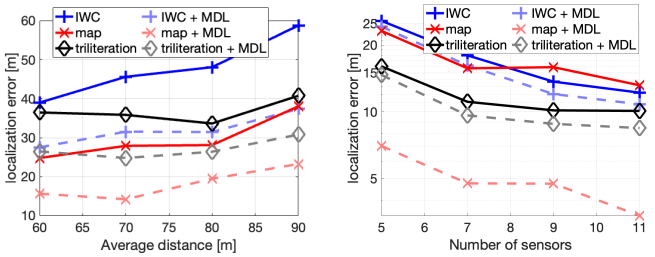

Figure 3: Localization accuracy when using the average PSD values of the sensor signal vs. the MDL-derived RSS proxy, with increasing average distance between transmitters and sensors (left), and the number of sensors (right).

We simulate the PSD observed at each sensor by sampling from a Gaussian distribution, which mimics the behavior of a WGN (White Gaussian Noise) channel. For each transmitter $t \in \{1, \ldots, N\}$, we generate PSD values using a normal distribution $\mathcal{N}_t(x \mid \mu_t, \sigma_t)$, where the mean μ_t corresponds to the received signal power computed via the log-normal model, and the standard deviation σ_t is set to 4 dB, informed by empirical measurements using a USRP B210 sensor. The resulting PSD traces from all sensors are stacked across time and frequency to form a third-order tensor $\mathcal{X} \in \mathbb{R}^{T \times F \times S}$, which serves as input to our framework.

Metrics. We evaluate MDL on three key tasks: time-frequency activity detection, spatial localization and transmitter count detection. For the *time-frequency activity detection*, we compute the *Jaccard similarity* between the detected activity and the ground truth for each transmitter. Since MDL separates each transmitter into a distinct tensor factor, we evaluate the detection performance per factor. Specifically, for each extracted component i, let $\mathbf{T}_i$ denote the binary detection (obtained via thresholded GMM on the time-frequency outer product), and let $\mathbf{G}_i$ be the corresponding ground truth activity mask. The Jaccard similarity for component i is given by:

$$J_i = \frac{|\mathbf{T}_i \cap \mathbf{G}_i|}{|\mathbf{T}_i \cup \mathbf{G}_i|} \text{ and } JS = \frac{1}{|N|} \sum_{i=1}^{N} J_i$$

Where JS is the final detection score computed by averaging over all transmitter components.

For the *localization task*, we measure the the Euclidean distance between the true transmitter coordinates and the predicted coordinates obtained from the proxy RSS vector and report the average across all transmitters.

For *transmitter count estimation*, we compare the number of predicted transmitters with the ground truth transmitter count.

Baselines. We compare MDL to one localization and two characterization baselines separately, since no existing method supports joint time-frequency-space characterization. For transmitter counting and time/frequency characterization we compare against SCAN [2] (using the authors' implementation) and CPD [20] (implemented in Matlab's tensor toolbox). Since SCAN operates on 2D matrices, we apply it to each frontal slice of our 3D tensor (corresponding to individual sensors) and average the results across all sensors. CPD provides a tensor decomposition baseline that differs from MDL primarily in its lack of structured dictionaries. To ensure fair comparison, we apply identical post-factorization processing as in MDL, substituting only the core decomposition method.

For localization, we compare our dictionary-derived proxy RSS vector against conventional approaches using average signal power per sensor. We use these as input to three established localization algorithms: Maximum A posteriori (MAP) [6], Interpolation-based Weighted Centroid (IWC) [11], and Triliteration. These methods represent different classes of power-based localization: probabilistic (MAP), interpolation-based (IWC), and geometric (Trilateration).

B. Results

Time-Frequency Activity Detection. We evaluate the performance of MDL in detecting the time-frequency activity of transmitters within a spectrum trace using a two-transmitter setup. First, we fix the number of active and inactive sensors to 5 and 4, respectively, and vary the average distance between the two transmitters and sensors from 50 m to 90 m. As shown in Fig. 2 (left), MDL achieves high detection accuracy across all distance settings, with a slight drop at 90 m due to the very low-SNR regime. On the other hand, SCAN and CPD show poor performance under these conditions. CPD consistently underperforms, while SCAN's accuracy falls off beyond 60 m.

Next, we fix the average transmitter to sensor distance at 90 m, resulting in low-SNR observations, and evaluate the benefit from increasing sensor density, as we increase the active sensors from 3 to 20. Fig. 2 (right) shows that MDL's detection accuracy improves with more sensors. This demonstrates MDL's ability to leverage spatial diversity to outperform both SCAN and CPD across all sensor configurations.

Localization using the proxy RSS vector. We evaluate the performance of our proxy RSS when compared to the average PSD value measured per sensor in localization task using MAP, IWC, and Triliteration. This evaluation is based on a single transmitter setting since the baselines (average signal power per sensor) cannot separate multiple transmitter signals, however, MDL naturally extends to multi-transmitter localization through its tensor decomposition, where each rank-1 factor isolates an individual transmitter's spatial signature.

First, we fix the number of active and inactive sensors to 5 and 4, respectively, and vary the average distance between transmitters and active sensors from 60 m to 90 m. As shown in Fig. 3 (left) we see that all the methods performed better while using the proxy RSS, than when not using it. Next, we

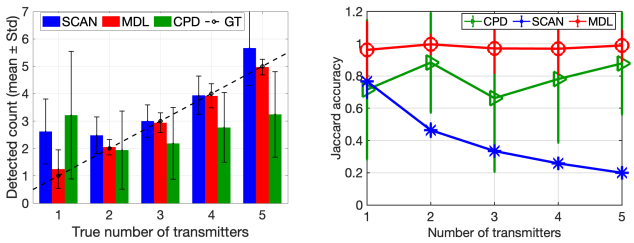

Figure 4: Performance with increasing number of transmitters: (Left) detected vs. true counts, (right) detection accuracy with increasing transmitters

fix the average transmitter to active sensor distance at 60 m and evaluate the impact of increasing sensor density. Specifically, we vary the number of active sensors from 5 to 11. Figure 3(right) also shows that the localization methods performed better while using the proxy RSS.

Performance with increasing transmitters. We next evaluate MDL under increasing numbers of transmitters. MDL decomposes multi-vantage measurements into distinct rank-1 components, each representing an individual transmitter. In this experiment, we fix the decomposition rank to $r_m = 10$, sensor count $S = 10$, average transmitter–sensor distance to 80 m, and vary the number of transmitters from 1 to 5. Fig. 4(left) shows the mean and standard deviation of detected transmitter counts across 200 trials. MDL closely matches the ground truth with low variance, whereas CPD and SCAN consistently over- or underestimate the counts. Fig. 4(right) confirms that MDL accurately captures both transmitter count and time–frequency activity. CPD improves as the true count approaches r_m, while SCAN's accuracy declines with more transmitters due to its single-vantage limitation and very low SNR per slice.

IV. Conclusion

We introduced MDL, a novel framework for joint transmitter characterization in time, frequency, and space via dictionary-based tensor factorization. Unlike traditional approaches that require separate measurement campaigns for different analytics task, MDL enables one-shot transmitter analytics, from a single multi-vantage wideband measurement. Experimental results demonstrate MDL's superior performance across all tasks. MDL isolates multiple transmitters into different components, accurately estimates transmitter counts, achieves robust time/frequency detection, and the dictionary derived proxy RSS vectors consistently gives an improved localization result. Notably, MDL is unsupervised, and technology-agnostic making it suitable for regulatory enforcement and spectrum sharing scenarios where transmitters of unknown characteristics must be detected and characterized, within multi-emitter environments.

References

[1] M. Zheleva, R. Chandra, A. Chowdhery, A. Kapoor, and P. Garnett, "TxMiner: Identifying transmitters in real-world spectrum measurements," in *2015 IEEE International Symposium on Dynamic Spectrum Access Networks (DySPAN)*, pp. 94–105, 2015.

[2] B. Okoro, M. McNeil, K. Meka, K. Doke, P. Bogdanov, and M. Zheleva, "Sparse recovery transmitter detection," in *IEEE INFOCOM 2025-IEEE Conference on Computer Communications*, pp. 1–10, IEEE, 2025.

[3] M. Khaledi, M. Khaledi, S. Sarkar, S. Kasera, N. Patwari, K. Derr, and S. Ramirez, "Simultaneous power-based localization of transmitters for crowdsourced spectrum monitoring," in *Proceedings of the 23rd annual international conference on mobile computing and networking*, pp. 235–247, 2017.

[4] S. Huang, Y. Yao, Z. Wei, Z. Feng, and P. Zhang, "Automatic modulation classification of overlapped sources using multiple cumulants," *IEEE Transactions on Vehicular Technology*, vol. 66, no. 7, pp. 6089–6101, 2017.

[5] A. Nika, Z. Li, Y. Zhu, Y. Zhu, B. Y. Zhao, X. Zhou, and H. Zheng, "Empirical validation of commodity spectrum monitoring," in *Proceedings of the 14th ACM Conference on Embedded Network Sensor Systems CD-ROM*, pp. 96–108, 2016.

[6] A. Bhattacharya, C. Zhan, A. Maji, H. Gupta, S. R. Das, and P. M. Djurić, "Selection of sensors for efficient transmitter localization," *IEEE/ACM Transactions on Networking*, vol. 30, no. 1, pp. 107–119, 2021.

[7] S. Sarkar, A. Baset, H. Singh, P. Smith, N. Patwari, S. Kasera, K. Derr, and S. Ramirez, "Llocus: learning-based localization using crowdsourcing," in *Proceedings of the Twenty-First International Symposium on Theory, Algorithmic Foundations, and Protocol Design for Mobile Networks and Mobile Computing*, pp. 201–210, 2020.

[8] C. Zhan, M. Ghaderibaneh, P. Sahu, and H. Gupta, "Deepmtl: Deep learning based multiple transmitter localization," in *2021 IEEE 22nd International Symposium on a World of Wireless, Mobile and Multimedia Networks (WoWMoM)*, pp. 41–50, 2021.

[9] A. Zubow, S. Bayhan, P. Gawłowicz, and F. Dressler, "Deeptxfinder: Multiple transmitter localization by deep learning in crowdsourced spectrum sensing," in *2020 29th International Conference on Computer Communications and Networks (ICCCN)*, pp. 1–8, IEEE, 2020.

[10] R. Bell, K. Watson, T. Hu, I. Poy, F. Harris, and D. Bharadia, "Searchlight: An accurate, sensitive, and fast radio frequency energy detection system," in *MILCOM 2023 - 2023 IEEE Military Communications Conference (MILCOM)*, pp. 397–404, 2023.

[11] S. Liu, Y. Chen, W. Trappe, and L. J. Greenstein, "Non-interactive localization of cognitive radios based on dynamic signal strength mapping," in *2009 Sixth International Conference on Wireless On-Demand Network Systems and Services*, pp. 85–92, IEEE, 2009.

[12] J. K. Nelson, M. R. Gupta, J. E. Almodovar, and W. H. Mortensen, "A quasi em method for estimating multiple transmitter locations," *IEEE Signal Processing Letters*, vol. 16, no. 5, pp. 354–357, 2009.

[13] Y. Zhang, T. Li, and Y. Zhang, "Gnn-sml: Graphic neural network-based spectrum misuser localization," in *IEEE INFOCOM 2025-IEEE Conference on Computer Communications*, pp. 1–10, IEEE, 2025.

[14] I. F. Akyildiz, B. F. Lo, and R. Balakrishnan, "Cooperative spectrum sensing in cognitive radio networks: A survey," *Physical communication*, vol. 4, no. 1, pp. 40–62, 2011.

[15] W. Lee, M. Kim, and D.-H. Cho, "Deep cooperative sensing: Cooperative spectrum sensing based on convolutional neural networks," *IEEE Transactions on Vehicular Technology*, vol. 68, no. 3, pp. 3005–3009, 2019.

[16] Z. Chen, Y.-Q. Xu, H. Wang, and D. Guo, "Federated learning-based cooperative spectrum sensing in cognitive radio," *IEEE Communications Letters*, vol. 26, no. 2, pp. 330–334, 2021.

[17] Z. Zhang, Y. Xu, J. Yang, X. Li, and D. Zhang, "A survey of sparse representation: algorithms and applications," *IEEE access*, vol. 3, pp. 490–530, 2015.

[18] D. Uvaydov, M. Zhang, C. P. Robinson, S. D'Oro, T. Melodia, and F. Restuccia, "Stitching the Spectrum: Semantic Spectrum Segmentation with Wideband Signal Stitching," in *IEEE INFOCOM 2024*, May 2024.

[19] F. L. Hitchcock, "The expression of a tensor or a polyadic as a sum of products," *Journal of Mathematics and Physics*, vol. 6, no. 1-4, pp. 164–189, 1927.

[20] B. W. Bader, T. G. Kolda, *et al.*, "Tensor toolbox for matlab," 2023.

[21] M. McNeil and P. Bogdanov, "Multi-dictionary tensor decomposition," in *2023 IEEE International Conference on Data Mining (ICDM)*, pp. 1217–1222, IEEE, 2023.

[22] M. Zheleva, P. Bogdanov, T. Larock, and P. Schmitt, "AirVIEW: Unsupervised transmitter detection for next generation spectrum sensing," in *IEEE INFOCOM 2018 - IEEE Conference on Computer Communications*, pp. 1–2, 2018.

[23] K. Doke, S. Sarkar, B. Okoro, D. Cabric, and M. Zheleva, "RadVIEW: Robust radar detection and characterization in high-noise regimes," in *IEEE DySPAN*, IEEE DySPAN, 2024.